Proceeding of the 17th ME-NETT Conference
15-17 October 2003, Prachinburi

Bone Stress Analysis of Dental Implants by Finite Element Method

Sutee OLARNRITHINUN*, Prarom SALIMEE** and Pramote DECHAUMPHAI*
*Department of Mechanical Engineering, Faculty of Engineering, Chulalongkorn University
**Department of Prosthodontics, Faculty of Dentistry, Chulalongkorn University
254 Payathai Road, Patumwan Bangkok 10330 Thailand
Tel: 0-2218-6621 Fax: 0-2218-6621 E-mail: fmepdc@eng.chula.ac.th

Abstract

The finite element method is used to study interfacial behavior inside biomaterials. The method and the contact constraints given as complemental conditions are performed by applying an augmented Lagrangian formulation for static two-dimensional frictionless contacts. Homogeneous material with no bonding between bones under linear elastic plane-strain condition are assumed. A finite element formulation and a corresponding computer program have been developed and validated by examples that have analytical solutions. Problems with complex geometry are presented to demonstrate the capability the finite element method for predicting detailed stress of dental implants.

1. Introduction

Dental implants are recently popular alternative to dentures. In general, dental implants restore the function of missing or removed teeth. They are anchored in the underlying alveolar bone while protruding through the socket into the oral cavity so as to provide abutment posts for single-tooth, fixed bridge or full arch appliances. As with their roles, dental implants undergo occlusal forces of various magnitudes and directions, some of which can be very large. Thus, the structural integrity and placement of implants are crucial for implant success.

Finite element analysis has been used recently in the field of orthopedic to investigate the stress transfer at the bone-implant interface for various designs. The use of the finite element analysis for structural mechanics of dental implants is ideal because it allows one to assess various parameters such as implant diameter, implant shape and load direction. All of these parameters play important roles in evaluating the efficacy of the dental implants. The principal difficulty in simulating the mechanical behavior of dental implants is the modeling of human bone tissue and its respond to applied mechanical forces. The substantial complexity of the mechanical characterization of bone and its interaction with implant systems has led to major and often incorrect simplification made in previous analyses, especially an assumption of bonding between bone and implant [1]. The contact between bone and implant is often modeled as a perfect bond, a situation exists in only a few cases. Therefore, the imperfect contact and its effect on the load transfer from implant to supporting bone need to be modeled more carefully. Typical mechanical behavior of bone-implant interface is similar to a material which exhibits a very low tensile and very high compressive pressure. Aware of this situation, contact problems have been applied to simulate the bone-implant interface which is used in orthopedic biomechanics studies [2]. The complexity in formulation arises due to the unknown contact surfaces and boundary conditions (displacements and contact forces) during loading.

In this paper, an augmented Largrangian formulation is used to solve small displacement frictionless contact behavior between deformable discretized bodies in two dimensions. The basic description and contact condition together with a finite element discretization of the two bodies are first defined in section 2. In section 3, the computational procedure of Usawa algorithm [6] is demonstrated. Validation of the contact model is presented in section 4 by comparing the predicted solutions with analytical solutions. Finally, applications of dental implant problems with complex geometry are presented to demonstrate the capability of the finite element method.

2. Theoretical formulation and solution procedure

2.1 Basic description and impenetrability constraint

The two bodies denoted by Ω^1 and Ω^2 as shown in Fig. 1 are defined as the *target* and *contactor*, respectively. The boundary of Ω^1 and Ω^2 are denoted by Γ^1 and Γ^2. At any time t, the boundary of each contact can be defined as,

$$\Gamma^n = \Gamma_D^n \cup \Gamma_F^n \cup \Gamma_C^n \qquad n=1,2 \tag{1}$$

where Γ^n denotes the total boundary of body n; Γ_D^n and Γ_F^n are parts of the boundary Γ^n for which the displacements and boundary loads are prescribed, respectively; and Γ_C^n is the part of boundary where contact may occur.

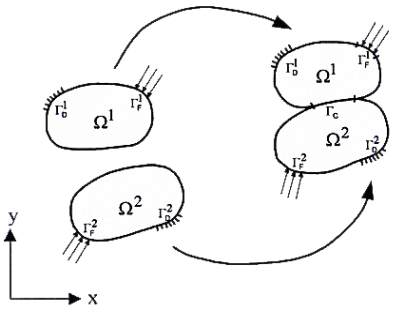

Fig. 1 Two bodies in contact system

The required conditions along the contact and the target surfaces are such that material overlapping cannot occur. As the result, contact forces are developed and act along the region of contact upon the target and the contactor. The normal tractions can only exert as compression action. The constraints normal to the contact surface can be expressed in terms of the following inequalities and equations that must be satisfied at each point on the contactor,

$$g_n \geq 0 \tag{2a}$$

$$t_n \leq 0 \tag{2b}$$

$$t_n \cdot g_n = 0 \tag{2c}$$

The first inequality (2a) represents the kinematic condition of no penetration of the contact surface. The second inequality (2b) is the static condition of compressive (or zero) normal tractions. The third equation (2c) states a complementary condition. If there is no contact, then no compressive traction can occur.

2.2 Variational formulation

The principal of virtual work, an equivalent formulation of the balance of momentum which often is called weak form of equilibrium, is used to formulate the contact behavior. For static contact problems, the virtual work can be written as,

$$\int_\Omega \boldsymbol{\sigma}\, \delta\mathbf{e}\, d\Omega - \int_{\Gamma_F} \bar{\mathbf{t}} \cdot \delta\mathbf{u}\, d\Gamma_F - \int_{\Gamma_C} t_n \mathbf{n} \cdot \delta\mathbf{u}\, d\Gamma_c = 0 \tag{3}$$

where $\boldsymbol{\sigma}$ is the stress vector, $\mathbf{e}$ is the infinitesimal strain vector, $\bar{\mathbf{t}}$ is the surface traction vector on Γ_F, t_n is the contact forces on Γ_C that have $\mathbf{n}$ as the unit surface normal vector and $\mathbf{u}$ is the displacement vector. The stress components are related to the strain components by the generalized Hook's law,

$$\boldsymbol{\sigma} = \mathbf{C}\mathbf{e} \tag{4}$$

The vector $\boldsymbol{\sigma}$ contains the stress components σ_x, σ_y and τ_{xy}, $\mathbf{C}$ is the material stiffness matrix [3]. The vector of the strain components is related to the displacement gradients given by,

$$\mathbf{e} = \left[\frac{\partial u}{\partial x} \quad \frac{\partial v}{\partial y} \quad \frac{\partial u}{\partial y} + \frac{\partial v}{\partial x} \right]^T \tag{5}$$

The contact constraint can be incorporated via different formulation into the general variational framework of the finite element method by the approach below.

2.3 Augmented Lagrangian formulation

The concept of the method [4-5] is based on modifying the contact term in equation (3),

$$\int_\Omega \boldsymbol{\sigma}\, \delta\mathbf{e}\, d\Omega - \int_{\Gamma_F} \bar{\mathbf{t}} \cdot \delta\mathbf{u}\, d\Gamma_F - \int_{\Gamma_C} (-\lambda_n + \varepsilon_n g_n(\mathbf{x})) \cdot \delta g_n(\mathbf{x})\, d\Gamma_c = 0 \tag{6}$$

where λ_n is Lagrange multiplier interpreted as the contact forces.

The approach between two discretized bodies is characterized, as shown in Fig. 2, by the following gap function,

$$g_n(\mathbf{x}) = \left[\mathbf{x}_s^2 - (1-\bar{\xi})\, \mathbf{x}_1^1 - \bar{\xi}\, \mathbf{x}_2^1 \right] \cdot \mathbf{n} \tag{7}$$

where g_n denotes the gap between two bodies normal to the target. From the above equation, $g_n(\mathbf{x}) > 0$ if a contact node has no penetration to the target segment. ε_n is known as the penalty parameter for the penalty regularization. An additional

variable Lagrange multiplier, λ_n, must be satisfied over Γ^n by the following condition,

$$-\lambda_n \leq 0 \tag{8}$$

The crucial idea in the method of augmented Lagrangian is to regard λ_n as a fixed current estimate of the correct Lagrange multiplier and then to solve,

$$\int_\Omega \boldsymbol{\sigma}\,\delta\mathbf{e}\,d\Omega - \int_{\Gamma_F} \bar{\mathbf{t}}\cdot\delta\mathbf{u}\,d\Gamma_F - \int_{\Gamma_C} < -\lambda_n^{(k)} + \varepsilon_n g_n(\mathbf{x}) > \cdot \delta g_n(\mathbf{x})\,d\Gamma_c = 0 \tag{9}$$

where $\lambda_n^{(k)} \geq 0$ denotes the fixed estimate of the correct λ_n. The subscript $(\,)^{(k)}$ reflects the fact that the search for the correct λ_n is an iterative process. One would suppose that it is good approximation to the correct multiplier, which motivates the update formula,

$$-\lambda_n^{(k+1)} = < -\lambda_n^{(k)} + \varepsilon_n g_n > \tag{10}$$

$< >$ is called the Macauley bracket, defined as $< x >= \frac{1}{2}\left[x - |x|\right]$. Its appearance in Eq. (9) is consistent with the interpretation of $-\lambda_n^{(k)} + \varepsilon_n g_n$ as the normal contact pressure, which must be negative.

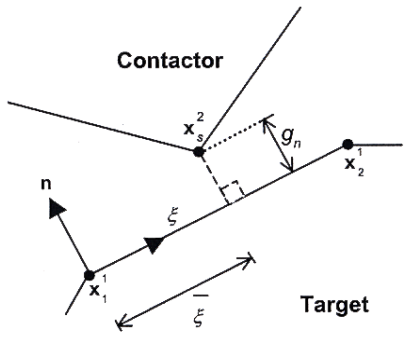

Fig. 2 Node-to-segment contact element.

2.4 Finite element formulation

It should be noted that Eq. (9) is nonlinear due to the nonlinear boundary conditions. Newton's method [6] is used to solve for solutions. The procedure is based on the Lagrangian description using the current configuration which leads to the updated Lagrangian formulation. The finite element equations corresponding to Eq. (9) can be written as,

$$\mathbf{G}(\mathbf{u}) = \mathbf{R}(\mathbf{u}) - \mathbf{P} - \mathbf{R}_c = 0 \tag{11}$$

Here the body Ω^n is discretized by n_e finite elements where,

$$\mathbf{R}(\mathbf{u}) = \bigcup_{e=1}^{n_e} \int_{\Omega_e} \mathbf{B}^T\boldsymbol{\sigma}\; d\Omega \tag{12}$$

$$\mathbf{P} = \bigcup_{e=1}^{n_e} \int_{\Gamma_e} \mathbf{N}^T\bar{\mathbf{t}}\; d\Gamma \tag{13}$$

$$\mathbf{R}_c = \sum_{e=1}^{n_c} < -\lambda_n + \varepsilon_n g_n > \cdot \mathbf{N}_S \tag{14}$$

where n_c is number of contact nodes on the boundary of contactor. **N** contains the shape functions and **B** is the strain displacement interpolation matrix. **R** denotes the stress divergence term or internal forces. $\mathbf{R}_c$ is the vector of contact forces and **P** is the load pattern.

For a known fixed Lagrange multiplier λ_n, the Newton's method is used to solve the nonlinear Eq. (11). The result, after linearization in the equation system at the state **u,** can be written as

$$\left[\mathbf{K}_T + \mathbf{K}_c\right]\{\Delta\mathbf{u}\} = -\mathbf{G}(\mathbf{u}) \tag{15}$$

where

$$\mathbf{K}_T = \bigcup_{e=1}^{n_e} \int_{\Omega_e} \mathbf{B}^T\mathbf{C}\mathbf{B}\; d\Omega \tag{16}$$

$$\mathbf{K}_c = \sum_{e=1}^{n_c} \varepsilon_n \mathbf{N}_S\mathbf{N}_S^T \tag{17}$$

$$\mathbf{N}_S = \left[\mathbf{n} \quad -(1-\bar{\xi})\cdot\mathbf{n} \quad -\bar{\xi}\cdot\mathbf{n}\right]^T \tag{18}$$

3. Computational procedure

From the previous section, the Lagrange multiplier is held constant during an iteration loop to solve the weak form in the inner loop. Then within an outer loop, the Lagrange multiplier is updated to a new value. This procedure is known as the Uzawa algorithm [6] with description as follows,

Initialize algorithm: $-\lambda_n^{(0)} = < -\lambda_n + \varepsilon_n g_n >$
from the last load step
Loop over augmentations: k=1, …, convergence
Loop over iterations: I=1, …, convergence
Solve: $\mathbf{G}(\mathbf{u}) = 0$ by Eq. (15)
Update displacement: $\mathbf{u}_{i+1} = \mathbf{u}_i + \Delta\mathbf{u}$
Check for convergence: $\|\mathbf{G}(\mathbf{u})\| \leq$ tol => end loop
End loop

Loop over contact node: n=1, …, n_c

Update : $-\lambda_n^{(k+1)} = < -\lambda_n^{(k)} + \varepsilon_n g_n >$

Check for convergence: $\left\| g_n(u) \right\| \leq$ tol => stop

End loop

End loop

4. Numerical results

Numerical results are presented in this section to demonstrate the validity of the described procedure. In these examples, small displacements and elastic deformation were assumed.

4.1 An elastic cylinder compressed by a rigid block onto a rigid foundation

An elastic cylinder compressed by a rigid block onto a rigid foundation as shown in Fig. 3 is used as the first example because its analytical solution is available. Due to symmetry, only one quarter of the cylinder was modeled as shown in Fig. 4. In this example, the total prescribed displacement was 1.35 mm. The calculated contact pressure distribution is shown in Fig. 5, for which the Hertzian solution [7] is also presented for comparison. The predicted radius of contacting area was 6.62 mm as compared to 6.87 mm by Hertzian solution.

4.2 Indentation of an elastic half-space by a rigid punch

The problem is depicted in Fig. 6 with the finite element mesh. For pressure load on the rigid punch of 0.328 GPa, contact pressure on the contacting area was solved and compared with the analytical solution [7] as shown in Fig. 7.

4.3 A screw thread problem

To evaluate the finite element formulation described on a more complex geometry, a screw thread problem as illustrated in Fig. 8 was used. The problem consists of the fixed and moving parts that have the same material property. The moving part has a prescribed displacement in the vertical direction. Figure 9 shows the predicted von Mises stress contours with high stress near the contact regions.

4.4 Bone stress distribution from dental implant

The finite element formulation was further evaluated on a more realistic problem of a bone stress analysis for dental implant. The problem statement, as shown in Fig. 10, consists of a titanium dental implant inserted in the cortical and cancellous bones. Detailed geometry of the implant teeth and material properties are shown in Fig. 10 and Table 1, respectively. A finite element mesh consisting of 2,230 nodes and 4,011 triangular elements with fine mesh in the teeth contact region is shown in Fig. 11. The predicted von Mises stress contours are shown in Fig. 12. The figure indicates that high stress occurs at the upper surface of the cortical bone near the dental implant.

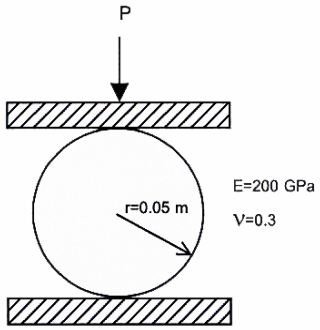

Fig. 3 A cylinder pressed by a rigid block onto a rigid foundation.

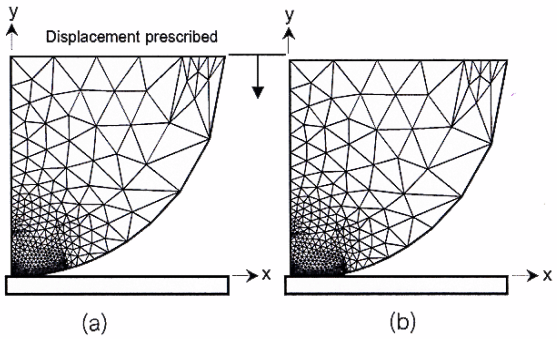

Fig. 4 (a) The finite element model for the cylinder.
(b) The deformed configuration of the cylinder.

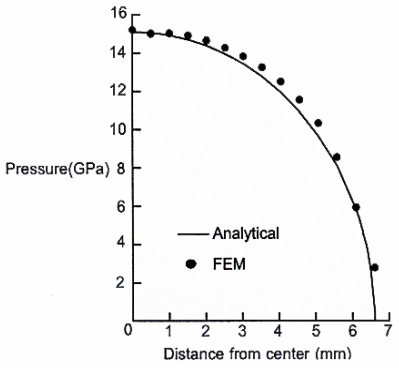

Fig. 5 Contact pressure distribution on a cylinder, where the horizontal axis is a distance from the center of cylinder.

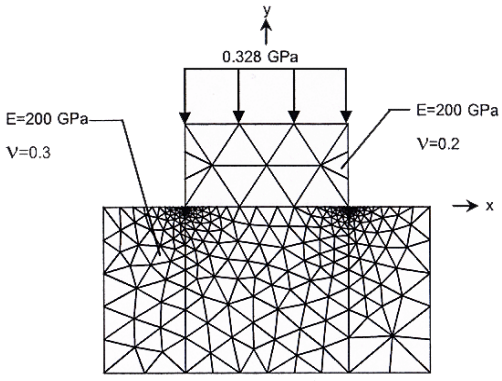

Fig. 6 Finite element mesh for the punch problem. Punch width =1 m and height =0.5 m.

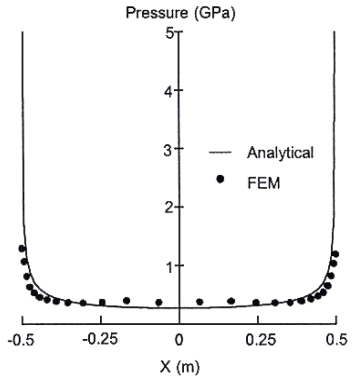

Fig. 7 Contact pressure distribute on the punch.

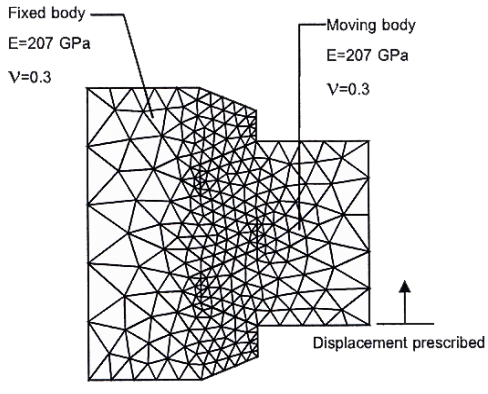

Fig. 8 Finite element mesh for the screw thread problem.

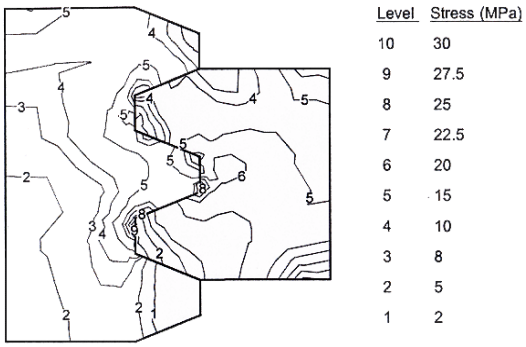

Fig. 9 Predicted von Mises stress contours for a screw thread problem.

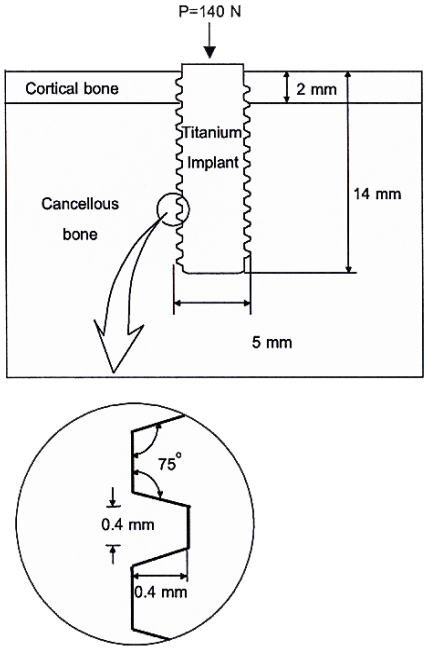

Fig. 10 The model of a dental implant and bone.

Materials	Young's modulus (E, GPa)	Poisson's ratio (ν)
Cortical bone	13.7	0.3
Cancellous bone	1.37	0.3
Titanium	103.4	0.33

Table 1 Properties of materials used in the model [8].

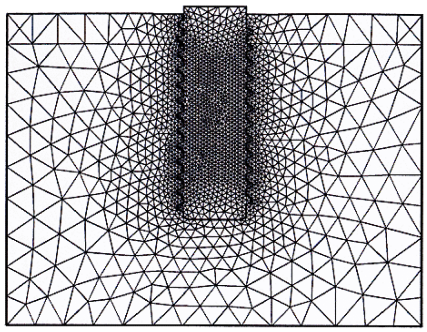

Fig. 11 Finite element mesh of dental implant and bone model.

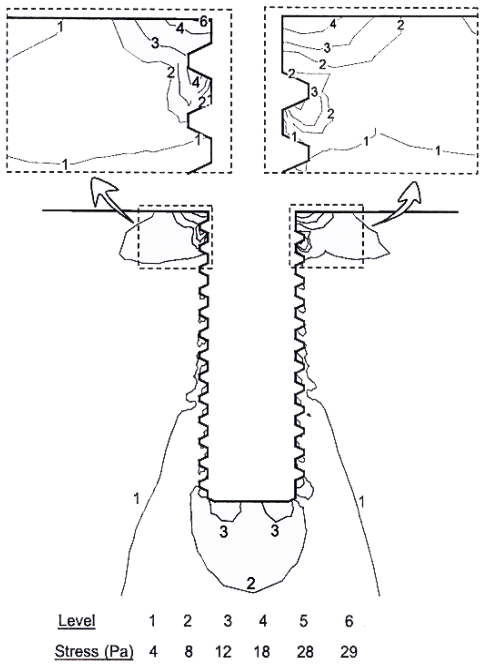

Fig. 12 Predicted von Mises stress contours in bone.

5. Conclusions

A finite element method was developed for studying the interfacial behavior inside biomaterials. The augmented Lagrangian formulation with Uzawa algorithm was implemented. Homogeneous materials with no bonding between the bone and dental implant under linear elastic plane-strain condition are assumed. A corresponding computer program has been developed and verified by examples for contact problems that have exact or analytical solutions. The developed finite element formulation and computer program were further evaluated on more complex problems with arbitrary geometry. Results show the capability of the finite element method that can provide inside of the detailed stress distribution of the bone and dental implants.

Acknowledgement

The authors would like to thank the Thailand Research Fund (TRF) for supporting this research work.

References

[1] Patra, K.A., DePaolo, J.M., D'Souza, K.S., Tolla, D.D. and Meenaghan, M.A., "Guidelines for Analysis and Redesign of Dental Implants", Implant Dentistry, Vol. 7, 1998, pp. 355-366.

[2] Viceconti, M., Muccini, R., Baleani, M. and Cristofolini, L., "On the Numerical Methods Used to Model Contact Between Prostheses and Host Bone", The Journal of Biomechanics, submitted on May 19, 1999.

[3] Dechaumphai, P., "Finite Element Method in Engineering", 2nd ed., Chulalongkorn University Press, Bangkok, 1999.

[4] Simo, J.C. and Laursen, T.A., "An Augmented Lagrangian Treatment of Contact Problems Involving Friction", Computer & Structure, Vol. 42, 1992, pp. 97-116.

[5] Heegaard, J.H. and Curnier, A., "An Augmented Lagrangian Method for Discrete Large-Slip Contact Problems', International Journal for Numerical Method in Engineering, Vol. 36, 1993, pp. 569-593.

[6] Wriggers, P., "Computational Contact Mechanics", John Wiley & Sons, 2002.

[7] Johnson, K.L., "Contact Mechanics", Cambridge University Press, Cambridge, 1985.

[8] Thanapalin, T., "The Effect of Different Shape and Thread Designs of Implant Fixture on Stress Distribution in Alveolar Bone: Finite Element Method", A Master Thesis, Department of Prosthodontics, Graduate School, Chulalongkorn University, 2001.

[9] Bathe, K.J. and Chaudhary, A., "A Solution Method for Planar and Axisymmetric Contact Problems", International Journal for Numerical Method in Engineering, Vol. 21, 1985, pp. 65-88.